

Preparation, Characterization and Low Frequency a.c. Conduction of Polypyrrole-Lead Titanate Composites

C. Basavaraja, Young Min Choi, Hyun Tae Park, Do Sung Huh,* Jae Wook Lee,[†]
M. Revanasiddappa,[‡] S. C. Raghavendra,[‡] S. Khasim,[‡] and T. K. Vishnuvardhan[§]

Department of Chemistry and Institute of Functional Materials, Inje University, Kimhae 621-749, Korea

*E-mail: chemhds@inje.ac.kr

[†]Department of Chemistry, Dong-A University, 840 Hadan-2-dong, Busan 604-714, Korea

[‡]Department of Chemistry, PES School of Engineering, Bangalore 560-100, India

[§]Department of Chemistry, Gulbarga University, Gulbarga 585-106, India

Received March 12, 2007

Conducting Polypyrrole-lead titanate (PPy/PbTiO₃) composites have been prepared by *in situ* deposition technique by placing different wt.% of fine grade powder of PbTiO₃ (10, 20, 30, 40, and 50%) during polymerization of pyrrole. The composites formed were characterized by X-ray diffraction (XRD), scanning electron microscopy (SEM), and thermogravimetric analysis (TGA), and these data indicate that PbTiO₃ particles are dominating with an increase in crystallinity as well as thermal stability of the composites. The results on the low frequency dielectric studies which are obtained in the form of pressed pellet state are interpreted in terms of Maxwell Wagner polarization, which are responsible for the dielectric relaxation mechanism and frequency dependence of conductivity.

Key Words : Composites, Polypyrrole, Conductivity, Dielectric behavior

Introduction

Conducting polymer composites have attracted considerable attention in recent past because of their numerous applications in a variety of electric and electronic devices. It has been found that such composites can exhibit several novel properties such as positive temperature coefficient of resistance and piezoresistivity.¹ The composites of conducting polymer with transition metal oxide (or sulfide) has been successfully prepared by several routes.² First one involves the concomitant intercalation and oxidative polymerization in a good oxidizing material such as V₂O₅.³ Alternatively, the monomer can be impregnated in the transition metal oxide (MoO₃)⁴ or sulfide (MoS₂)⁵ host and subsequently undergoes polymerization upon exposure to an external oxidizing agent. Polyaniline-Fe_xO_y composites were obtained by reacting the emeraldine base form of polyaniline with an aqueous solution of iron sulfate.⁶ Finally, the co-electro deposition of analogous composites has been also reported.^{7,8} And also, polypyrrole has been prepared with MoS₃⁹ by D. Bélanger *et al.* and others have incorporated oxides such as MnO₂, TiO₂, and WO₃ into polypyrrole (PPy).⁸ These composites act as potential cathode materials for rechargeable lithium batteries and in electrochromic displays. In addition, these conducting polymers are known to increase conductivity after polymerization in the presence of the commonly highly resistive oxide or sulfide and improve the redox capacity of the battery.⁸

Preparation of these polymer composites in the presence of insulating materials is useful in improving the electrical properties, morphology, stability and crystal structure of these composites which are the key factors in governing the

device performance. One way of making these composites involves synthesizing the conducting polymers using chemical or electrochemical polymerization in the presence of such materials.^{7,8} In this study PPy/PbTiO₃ composites have been prepared by *in situ* deposition technique by placing different wt. % of fine grade powder of PbTiO₃ (10, 20, 30, 40, and 50%) during *in situ* polymerization of pyrrole. The interfacial interactions and thermal stability of these composites are characterized by XRD, SEM and TGA techniques. Low frequency dielectric studies were carried out on pressed pellets and the origin of electrical properties of these composites have been studied in the context of polymer-oxide interactions.

Experimental

Materials. Analytical grade pyrrole, lead titanate, and ammonium per sulfate were obtained from Aldrich. Pyrrole was purified by distillation under nitrogen flow and was kept in the dark prior to use.

Preparation of PPy and PPy/PbTiO₃ composites. 0.03 M of distilled pyrrole was added to the solution of 0.06 M ammonium per sulfate and the reaction mixture was stirred continuously at a constant temperature (5 °C) to obtain PPy. To this reaction mixture, varied weight percent (10, 20, 30, 40, and 50) of lead titanate as a fine powder was added to form pyrrole-lead titanate composites. The obtained product was filtered and washed thoroughly with methanol (CH₃OH) and the sample was dried under vacuum for more than 24 h at room temperature.

Measurements. The FT-IR spectra of the samples were measured by a Perkin Elmer (model 783) IR spectrometer in

KBr medium at room temperature. The SEM images of pure PPy and PPy/PbTiO₃ (30 wt %) were investigated using XL-30 ESEM scanning electron microscope. The X-ray diffraction patterns of the samples were recorded using Philips X-ray diffractometer using CuK α radiation ($\lambda = 1.5406 \text{ \AA}$). The diffractograms were recorded in terms of 2θ in the range of 10° - 80° with a scanning rate of 2° per min. Thermal properties were obtained by thermogravimetric analysis (Perkin Elmer model TGA 7) in the temperature range from 20 to 800°C at a heating rate of $10^\circ\text{C}/\text{min}$ under nitrogen atmosphere. Dielectric measurements of these composites were carried out in the frequency range of 10^2 - 10^6 Hz using the Hewlett-Packard impedance analyzer 4192 A model at room temperature. The test samples to be used were prepared in pellet form of diameter 10 mm and thickness 3 mm by applying pressure of 9 M Pa. Silver paste is coated and a copper wire is attached on both sides to obtain a better contact during the impedance measurement.

Results and Discussion

FT-IR spectra. Figures 1a, 1b, and 1c show the IR spectrum of pure PbTiO₃, pure PPy, and PPy/PbTiO₃ (30%), respectively. Figure 1a shows the FT-IR spectra for pure PbTiO₃, and the bands at 713 cm^{-1} and 387 cm^{-1} indicate the presence of metal oxygen stretching, which in turn implies the presence of a metal oxygen bond. In Figure 1b, the bands at 1306 cm^{-1} and 1180 cm^{-1} may correspond to =C-H in plane vibration, while the peaks at 782 cm^{-1} and 902 cm^{-1} are due to =C-H caused by an out of plane vibration.¹⁰ The

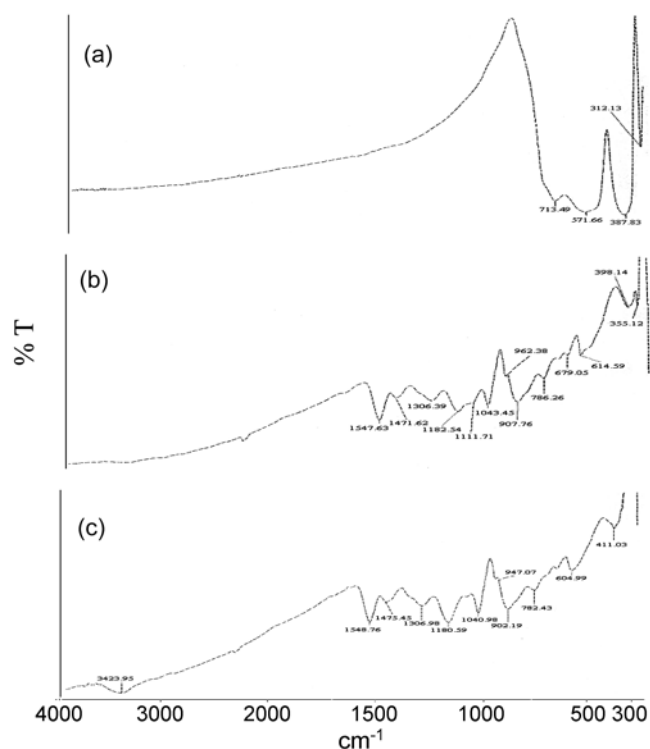


Figure 1. FTIR spectra of (a) pure PbTiO₃, (b) pure PPy, and (c) PPy/PbTiO₃ (30 wt %).

peak observed around 1040 cm^{-1} is for the C-H vibration of 2,5-substituted pyrrole.¹¹ The bands for pure PPy at 1548 cm^{-1} are due to intra ring C=C and inter ring C-C vibration,¹⁰ which are comparatively higher than its composite ca. 1547 cm^{-1} as shown in Figure 1c. This is due to the shifting of bands towards a lower wavelength after composite formation, which indicates the shortening of the PPy chain.¹¹ Meanwhile, Figure 1c shows the FT-IR of a PPy/PbTiO₃ (30 wt %) composite sample. The band at 1471 cm^{-1} indicates the combination of the intra ring C=C and the inter ring C-C vibration in the composite samples.¹² The characteristic IR peak observed at 1182 cm^{-1} may be due to the =C-H in plane vibration, and the peaks around 786 cm^{-1} and 907 cm^{-1} may be =C-H out of plane vibration.¹³ These bands are also called bipolaron bands.¹¹ The bands around 1043 cm^{-1} may be due to the C-H vibration of 2,5-substituted PPy^{14,15} which indicates the presence of polymerized (or oxidized) pyrrole in the composites. The IR spectra of other composites (PPy with 10, 20, 40, and 50 wt % of PbTiO₃) show similar absorption peaks without much variations in their stretching frequencies. This shows that there is a weak interaction between the metal and polymer components of the composite.

Pattern of X-ray diffraction. Figure 2 shows X-ray diffraction patterns of PPy/PbTiO₃ (10 wt % of PbTiO₃), PPy/PbTiO₃ (30 wt %), and PPy/PbTiO₃ (50 wt %), respectively. XRD patterns of PPy/PbTiO₃ composites exhibit a predominant PbTiO₃ peaks than PPy. By comparing the X-ray diffraction patterns of composites with those of PbTiO₃, the peaks at 31.72° have been assigned to the (110) plane of perovskite structure and the one at 56.40° to the (222) plane of pyrochlore structure, as could be noted from the respective JCPDS (in 00-002-0804) files. This may be caused by the scattering of PPy chains at the interplanar spacing¹⁶ due to the encapsulation of PPy on the PbTiO₃ particles.

Scanning electron microscopy. SEM micrographs of the pure PPy and PPy/PbTiO₃ (50 wt %) composites are display-

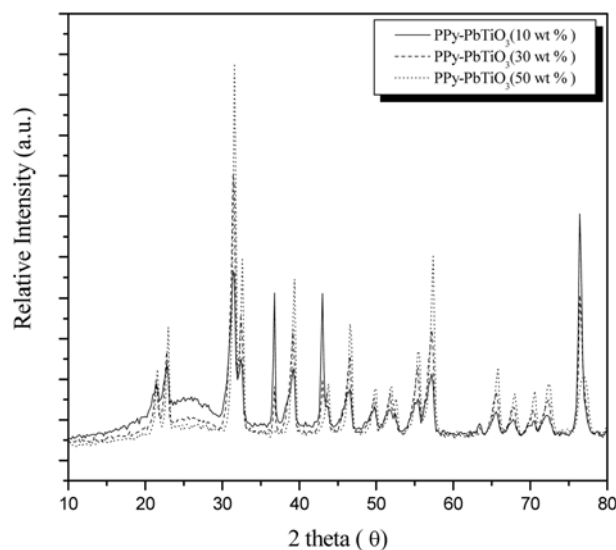


Figure 2. XRD patterns of PPy/PbTiO₃ (10 wt %), PPy/PbTiO₃ (30 wt %), and PPy/PbTiO₃ (50 wt %).

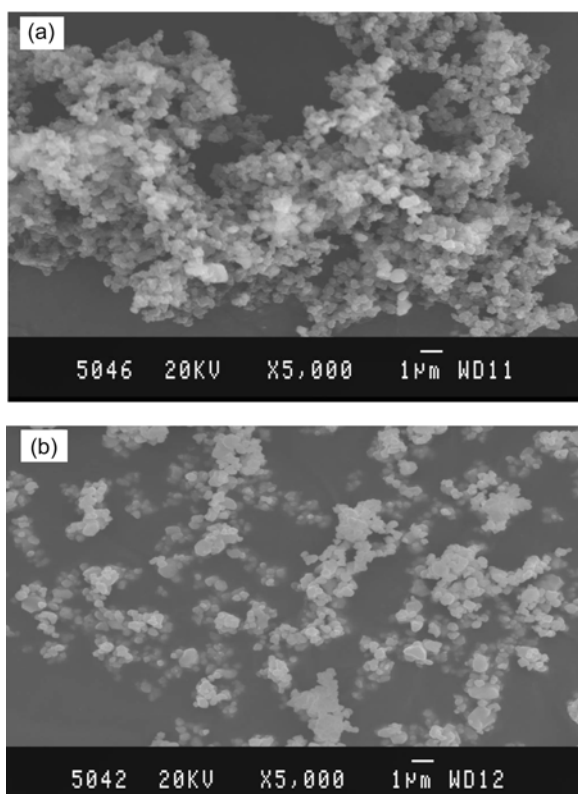


Figure 3. Scanning electron micrographs of (a) pure PPy and (b) PPy/PbTiO₃ (50 wt %).

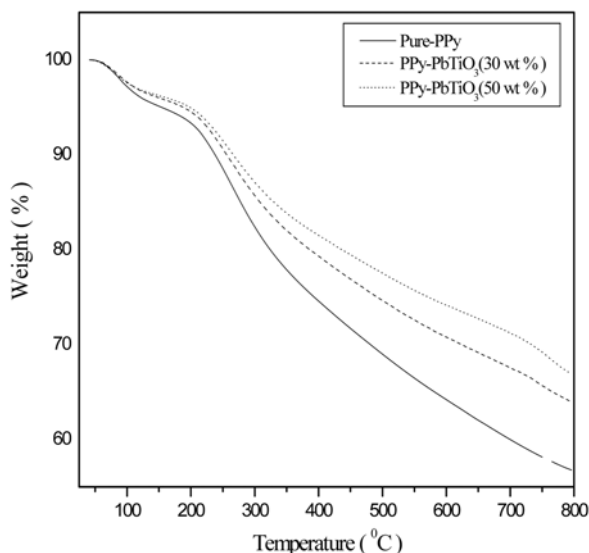


Figure 4. TGA curves obtained from PPy, PPy/PbTiO₃ (30 wt %), and PPy/PbTiO₃ (50 wt %).

ed in Figure 3. Pure PPy (Figure 3a) shows an aggregated structure, while PPy/PbTiO₃ (50 wt %) composite (Figure 3b) exhibits an aggregated granular morphology. With increasing the amount of PbTiO₃ (20, 30 and 40 wt %), larger size aggregates are visible as shown in Figure 3. It suggests intermixing of PbTiO₃ particles with the PPy matrix.

Thermogravimetric analysis. Thermal degradation patterns for PPy, PPy/PbTiO₃ (30 wt %) and PPy/PbTiO₃ (50

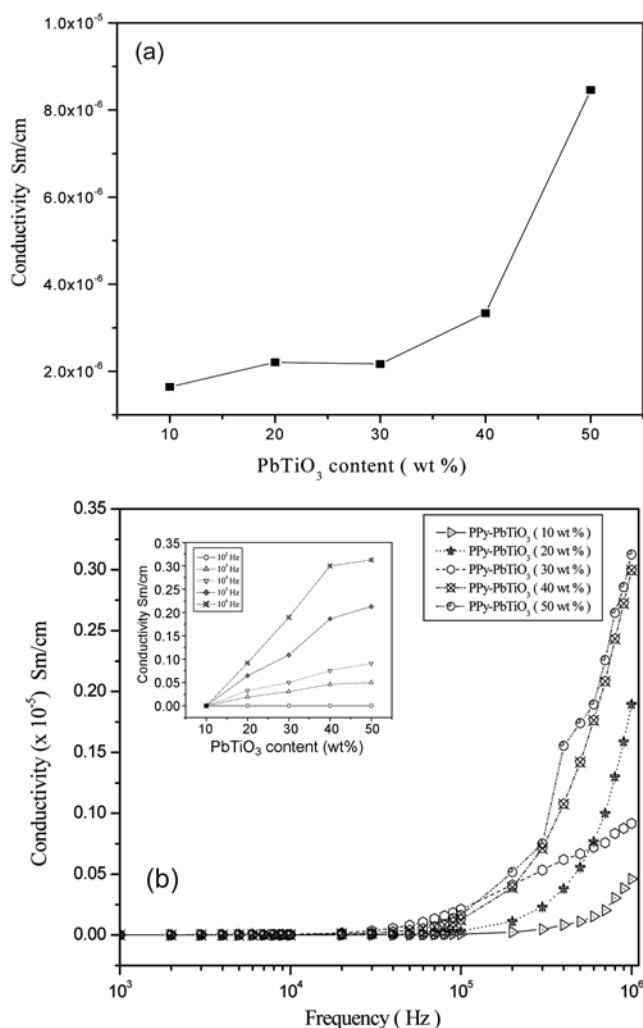


Figure 5. Frequency dependence of a.c. conductivity of PPy/PbTiO₃ composites. (a). Variation of conductivity of PPy/PbTiO₃ at different frequency with PbTiO₃ content in the composite (b). At different frequency with increase in the content of PbTiO₃ in the composite (Inset: The conductivity of PPy/PbTiO₃ composites for different wt % of PbTiO₃ at different frequencies).

wt %) are shown in Figure 4, respectively. PPy and PPy/PbTiO₃ composites show a three stage decomposition pattern. The first stage ranging from room temperature to 100 °C corresponds to a loss of water molecules/moisture present in the polymer. The second stage from 120 to 320 °C is associated with a loss of dopant ion from the polymer matrix. However, the weight loss after 320 °C is due to complete degradation and decomposition of the polymer after the loss of dopant ion.¹⁷ PPy showed a weight loss of 56% up to 800 °C, which increased after the introduction of PbTiO₃ into PPy. The PPy/PbTiO₃ (30 wt %) matrix showed a weight loss of 63%, which further increased to 66% for PPy/PbTiO₃ (50 wt %) composite. This fact confirms that PbTiO₃ has a positive influence on the thermal stability of composites, in other words PbTiO₃ inhibits a fast degradation of the polymers.

Studies on the electrical conductivity. Frequency-dependent a. c. electrical conductivities of PPy/PbTiO₃ obtained at

room temperature are shown in Figure 5 and the inset figure shows those of composites with an increase in the wt % of PbTiO_3 . These composites show similar behavior up to 10^4 Hz, viz. that there is no significant variation in the conductivity with frequency during this range. Further as the frequency is increased further, conductivity goes on increasing. The most important and interesting observation is that, the conductivity of all composites are significantly higher with increasing PbTiO_3 , in spite of the fact that PbTiO_3 is an insulating material at room temperature. Since the synthesized condition of these composites is same, the microscopic conductivities of all composites should remain same. However, the macroscopic properties viz. compactness and molecular orientations may significantly vary due to the variations in the weight percentage of PbTiO_3 in composites. During the polymerization process there is a distribution of small crystalline particles of PbTiO_3 in the polymer matrix which are homogeneously distributed there by decreasing the specific surface area of the polymer matrix in the composites due to clustering of salt particles. This brings to an increase in the orderness in the composites, as it can be confirmed by Figure 1, 2 and 3. The increase in orderness, compactness and molecular orientations, leads to an increase in macroscopic conductivity of the composites.

The increase in the conductivity values of PPy/ PbTiO_3 with the increase in wt % of PbTiO_3 can be qualitatively compared to that of the PPy/ Y_2O_3 composites.¹⁸ This can be considered specifically due to the improvement in the weak links between the polymer and the oxide particles which resulting in a stronger coupling through the grain boundary.¹⁹ Pure PPy is very light with poor compactness since microparticles are randomly oriented and the linkage among the polymer particles is very weak, resulting in relatively lower conductivity.²⁰ In comparison, the presence of PbTiO_3 in the composites helps the formation of a granular shape, which leads to an improvement in the compactness of the composite materials. As PbTiO_3 content in composites increases, the change in compactness becomes more significant due to an improvement of weak links between grains due to the encapsulation of polymer on the salt. This ultimately results in an improvement in macroscopic conductivity.

Dielectric behavior. The frequency-dependent dielectric constant and dielectric losses of pure PPy and PPy/ PbTiO_3 composites at room temperature are plotted in Figures 6 and 7, respectively. The inset of both figures shows the dielectric constant and dielectric loss of PPy/ PbTiO_3 composites at different frequencies with an increase in the wt % of PbTiO_3 . Dielectric constant decreases as the frequency is increasing and this remains nearly same after the frequency of 10^4 Hz. The value of dielectric constant is smaller for the composites with lower content of PbTiO_3 (10% and 20%) and it increase somewhat in the composite with 30 wt % of PbTiO_3 , however further increase in PbTiO_3 content decreases the dielectric constant of the composite. As one can see from Figures 5 and 6 that dielectric constant and dielectric loss values are higher due to the higher content of the oxide in

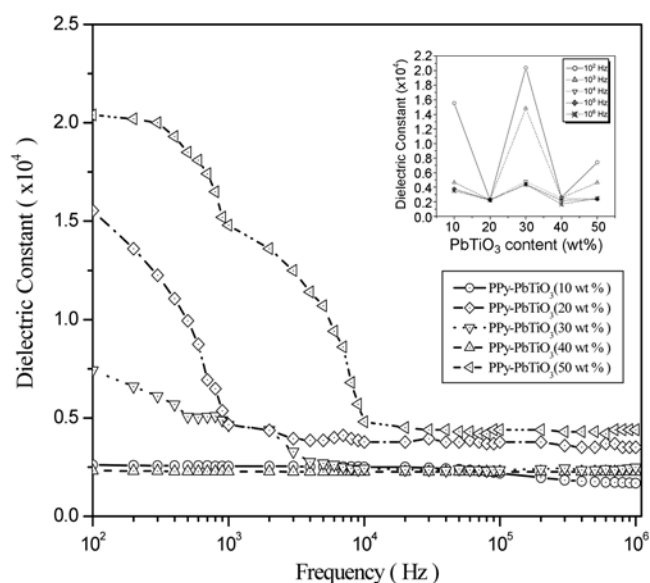


Figure 6. Frequency-dependent dielectric constant of PPy/ PbTiO_3 composites (Inset: Dielectric constant of PPy/ PbTiO_3 composites for different wt % of PbTiO_3 at different frequencies).

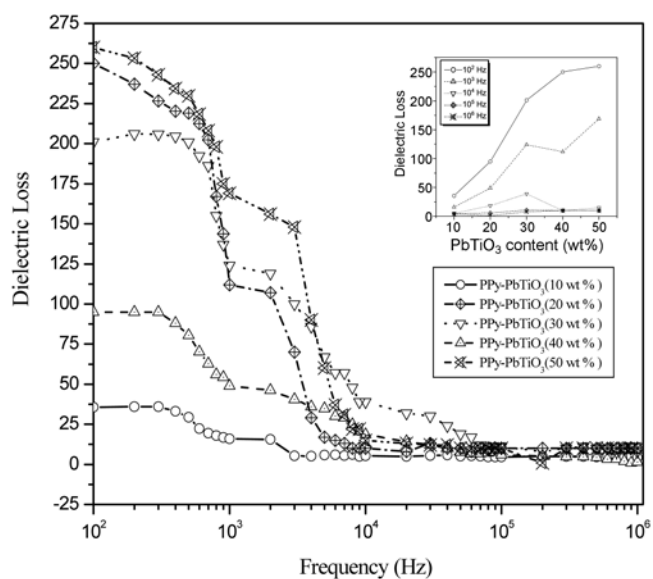


Figure 7. Frequency-dependent dielectric loss of PPy/ PbTiO_3 composites (Inset: Dielectric loss of PPy/ PbTiO_3 composites for different wt % of PbTiO_3 at different frequencies).

these composites. It is evident from Figures 5, 6, and 7 that conductivity behavior and the dielectric properties of these composites are opposite in nature.

A higher dielectric constant and dielectric loss for a higher content of PbTiO_3 can be interpreted by an increase in crystallinity due to clustering of PbTiO_3 particles in the polymer matrix; this can be confirmed from XRD and micrographs. The resulting orderness in these composites increases the interfacial interactions between the polymer and the PbTiO_3 , leading to maximum space charge polarization.¹³ In the Maxwell Wagner two-layered model, the dielectric function depends on the conductivity and permitti-

vity of the two layers. Here, the dielectric constant arises due to static dielectric permittivity (ϵ_s) which can be given as

$$\epsilon_s = C_{gb} / C_0$$

where C_0 is the capacitance under vacuum. This equation demonstrates that the dielectric constant which mainly depends on grain boundary capacitance (C_{gb}). The grain conductivity decreases with increase in $PbTiO_3$ concentration, the charge carrier concentration decreases resulting in a decrease in grain boundary capacitance. Hence the reduction of grain boundary capacitance and grain size gives rise to a decrease in dielectric constant. For pure PPy, highest conductivity and dielectric loss behavior may be due to the free motion of the charge carriers. In case of composites, while oxide content is less (*i.e.* 10%) in the polymer the interface between the polymer and grain is poor leading to decrease in conductivity and dielectric behavior. As the oxide content is more (*i.e.* 50%) in the polymer composite, orderness increases, so packing density increases, interface between the polymer and oxide is more leading to maximum space charge polarization (Maxwell Wagner polarization) contributing to highest dielectric behavior.

Conclusion

PPy/ $PbTiO_3$ composites were prepared by dispersing different amounts of $PbTiO_3$ particles in a polypyrrole matrix. The FT-IR spectral peaks of PPy/ $PbTiO_3$ composite (with 30 wt % $PbTiO_3$) show presence of oxide in the polymer though $PbTiO_3$ in the composites does not effectively involve chemically with PPy. But weak interaction with oxide and PPy may contribute to the conductivity and dielectric behavior. The SEM images and XRD patterns of PPy/ $PbTiO_3$ showed more orderness due to aggregation of particles as well as particle agglomeration as compared to pure PPy, and this increase in stability of these composites was confirmed by TGA. The increase in the a.c. conductivity of PPy/ $PbTiO_3$ composites over pure PPy was due to macroscopic conductivity and the frequency-dependent dielectric constant is on the basis of dielectric mechanism. The increase in orderness may be attributed to the occurrence of packing density and maximum space charge (Maxwell

Wagner) polarization, which in turn resulted in the increase in electrical properties of these composites. Dielectric loss resulted due to the localized motion of charge carriers resulting high values of dielectric loss compared to pure PPy. The improvements made in properties of these composites are expected to enhance the application potential of the polymer without altering its chemical properties.

Acknowledgment. This work was supported by Inje Research Scholarship.

References

1. Novak, P.; Muller, K.; Santhanam, K. S. V.; Hass, O. *Chem. Rev.* **1997**, *97*, 207.
2. Fusalba, F.; Belanger, D. *J. Mater. Res.* **1999**, *14*(5), 1805.
3. Wu, C. G.; Degroot, D. C.; Marcy, H. O.; Schinder, J. L.; Kannewurf, C. R.; Liu, Y. J.; Hipro, W.; Kanatzidis, M. G. *Chem. Mater.* **1996**, *8*, 1992.
4. Kerr, T. A.; Wu, H.; Nazar, L. F. *Chem. Mater.* **2005**, *8*, 1996.
5. Wang, L.; Schindler, J.; Thomas, J. A.; Kannewurf, C. R.; Kanatzidis, M. G. *Chem. Mater.* **1995**, *7*, 1753.
6. Wan, M.; Shou, W.; Li, J. *Synth. Met.* **1996**, *78*, 27.
7. Ahn, S.; Hupp, J. T. *Bull. Korean Chem. Soc.* **2006**, *27*(9), 1497.
8. Gemeay, A. H.; Nishiyama, H.; Kuwabata, S.; Yoneyama, H. *J. Electrochem. Soc.* **1999**, *142*, 226 and references therein.
9. Girard, F.; Ye, S.; Laperriere, G.; Belanger, D. *J. Electroanal. Chem.* **1992**, *334*, 35.
10. Maxwell, C. J. *A Treatise on Electricity and Magnetism*; Oxford University Press: Oxford, 1998; Vol. 1, p 285.
11. Belez, F. A.; Zarbin, A. J. G. *J. Braz. Chem. Soc.* **2001**, *12*(4), 542.
12. Chwang, C. P.; Liu, C. D.; Huang, S. W.; Chao, D. Y.; Lee, S. N. *Synth. Met.* **2004**, *142*, 275.
13. de Azevedo, W. M.; de Souza, J. M.; De Melo, J. V. *Synth. Met.* **2001**, *124*, 295.
14. Suri, K.; Annapoorani, S.; Tandon, R. P.; Mehra, N. C. *Synth. Met.* **2002**, *126*, 137.
15. Bhattacharyya, S.; Saha, S. K.; Mandal, T. M.; Mandal, B. M.; Chakravorty, D.; Goswami, K. J. *J. Appl. Phys.* **2001**, *89*, 5547.
16. Kalinichev, A. G.; Bass, J. D. *J. Mat. Res.* **1997**, *12*(10), 2623.
17. Patil, S. F.; Bedekar, A. G.; Agashe, C. *Mater. Lett.* **1992**, *14*, 307.
18. Vishnuvardhan, T. K.; Kulkarni, V. R.; Basavaraja, C.; Raghavendra, S. C. *Bull. Mater. Sci.* **2006**, *29*(1), 77.
19. Chil-Hoon Doh; Seong II Kim; Ki-Young Jeong; Bong-Soo Jin; Kay Hyeok An; Byung Chul Min; Seong-In Moon; Mun-Soo Yun, *Bull. Korean Chem. Soc.* **2006**, *27*(8), 1175.
20. Cohen, R. E. *Nature* **1992**, *358*, 136.